PROCEEDINGS, 51st Workshop on Geothermal Reservoir Engineering
Stanford University, Stanford, California, February 9-11, 2026
SGP-TR-230

Influence of Thermal Properties Heterogeneity on Geothermal Production and Fracture Spacing for Enhanced Geothermal System

Pengju Xing[1,2], Clay Jones[1], Branko Damjanac[3], Stuart Simmons[1], Joseph Moore[1], Milind Deo[1,4], John McLennan[1,4]

1 Energy & Geoscience Institute, University of Utah, Salt Lake City, UT, USA

2 Department of Civil and Environmental Engineering, University of Utah, Salt Lake City, UT, USA

3 Itasca Consulting Group, Minneapolis, MN, USA

4 Department of Chemical Engineering, University of Utah, Salt Lake City, UT, USA

Keywords: Thermal properties heterogeneity, geothermal production, Enhanced Geothermal System

ABSTRACT

Enhanced Geothermal Systems (EGS) rely on efficient heat transfer between circulating fluids and hot rock through engineered fracture networks. Reservoir thermal properties—particularly thermal conductivity and specific heat capacity—play a critical role in production temperature, thermal power output, and fracture spacing. These thermal properties are commonly assumed to be homogeneous, yet laboratory measurements from Utah FORGE core and cuttings reveal substantial spatial and temperature-dependent heterogeneity. Core and cutting analyses show that thermal conductivity can vary by up to 67% along depth, largely driven by mineralogical differences, especially quartz content. In addition, thermal conductivity decreases while specific heat capacity increases with increasing temperature, leading to reduced thermal diffusivity at reservoir conditions. This study integrates laboratory measurements with numerical simulations to quantify the influence of thermal property heterogeneity on EGS performance. Numerical simulation results of both single-fracture and multi-fracture doublet systems demonstrate that a 50% increase in thermal conductivity combined with a 20% increase in heat capacity can increase produced thermal power by approximately 11%. In heterogeneous reservoirs, the presence of a 130 m high thermal property layer enhances thermal power output by 3.6%. Furthermore, reduced thermal diffusivity at elevated temperatures decreases the fracture spacing required to maintain thermal independence, lowering fracture spacing from approximately 100 m to 85 m for a 30-year project lifespan. These results highlight the importance of incorporating realistic thermal property heterogeneity into EGS design and performance assessments.

1. INTRODUCTION

Enhanced Geothermal System (EGS) production relies on heat transfer between circulated fluid and hot rock through engineered fracture networks. The longevity and production temperature of EGS are influenced by the thermal properties of the reservoir, including thermal conductivity and specific heat capacity. In addition, for EGS, to avoid heat interference between fractures a minimum spacing between fractures is required, and this spacing depends on the reservoir thermal properties. These thermal properties are often assumed to be homogeneous within geothermal reservoirs. However, laboratory testing data from Utah FORGE reveal significant variability. The thermal conductivity and specific heat capacity vary due to different mineral components at EGS reservoir (e.g., Utah FORGE, see Jones et al., 2024). Thermal properties depend not only on mineralogical composition but also on temperature. The laboratory data shows that thermal conductivity decreases while specific heat capacity increases with increasing temperature, leading to a reduction in thermal diffusivity at elevated temperatures for constant rock density.

Heterogeneity in thermal properties affects both production temperature, rock temperature evolution, and the designing fracture spacing during reservoir stimulation. In this study, we first present laboratory measured thermal properties from the core and cuttings from Utah FORGE wells. Then, we conducted numerical simulations of heat transfer in and EGS doublet under various homogeneous and heterogeneous thermal properties, considering cases with single fracture and multiple fractures. Production temperature, thermal power output, and required spacing to avoid heat interference among fractures are compared across these cases.

2. THERMAL PROPERTIES HETEROGENEITY

2.1 Core testing data

Thermal properties including thermal conductivity and heat capacity were measured on core samples from Utah FORGE wells 58-32 and 16A(78)-32 (MetaRock Laboratories, 2021). These results are summarized in Table 1. The three samples have densities of 2.68, 2.60, and 2.65 g/cc, respectively, indicating minimal variability.

Table 1: Thermal properties of core samples from FORGE wells 58-32 and 16A(78)-32

Temperature (°C)	Heat capacity [J/(kg·K)]			Thermal conductivity [W/(m·K)]		
	58-32A (7440.43 ft)	16A(78)-32	58-32B (6803.989 ft)	58-32A (7440.43 ft)	16A(78)-32	58-32B (6803.989 ft)
35	798.7	785.8	988.2	2.165	2.389	3.087
100	864.8	862.3	1091.1	2.149	2.341	3.002
200	981.3	944.5	1175.2	2.041	2.206	2.672

The measurements show that the specific heat capacity increases with temperature whereas thermal conductivity decreases with temperature (e.g. sample 58-32B plotted in **Figure 1**), leading to a reduction in thermal diffusivity at elevated temperatures for constant density. Similar trends have been reported in the literature (e.g. Heuze, 1983, and Walsh and Decker, 1966). The testing data also reveal significant variability among different samples. For example, at 200 ºC, the thermal conductivity in the most conductive sample – 58-32B is ~30% higher than in the least conductive sample – 58-32A, while specific heat capacity is also ~20% higher. Notably, the core sample 58-32B exhibits both the highest conductivity and the highest specific heat capacity.

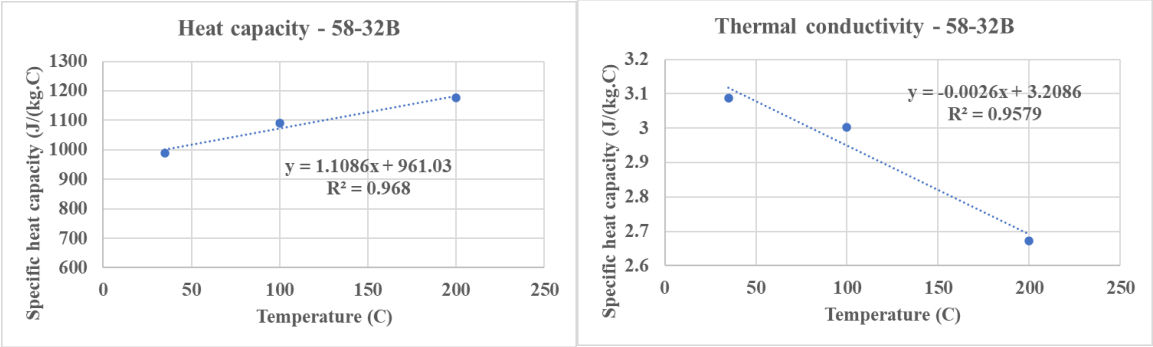

Figure 1. Heat capacity and thermal conductivity vs. temperature for core sample 58-32B.

Table 2 summaries the Xray Diffraction (XRD) results of core samples from well 58-32. The XRD results of sample X-2 can present sample 58-32B because their measured depth (MD) is close; similarly, sample X-5 is used to represent sample 58-32A. The mineral components of 58-32A(X-5) are quite different from 58-32B(X-2): 58-32B(X-2) contains less plagioclase, biotite, and hornblende, but substantially more K-feldspar and quartz. The photos of core sample 58-32A and 58-32B are shown in **Figure 2**. Literature laboratory testing data (Horai, 1971; Cho et al., 2009)) shows that thermal conductivity of quartz is 7.7 W/(m.K), which is significantly higher than other common rock minerals such as plagioclase (1.8 W/(m.K)) and biotite (2.1 W/(m.K)). This explains that the higher thermal conductivity of sample 58-32B is due to its greater quartz content.

Table 2: XRD results of core samples from well 58-32 at Utah FORGE (Nash and Jones, 2018)

Sample ID	MD (ft)	Plagioclase	K-feldspar	Quartz	Biotite	Titanite	Hornblende	Apatite	Smectite	Interlayered Chlorite-Smectite	% chlorite in C/S	Chlorite	Illite	Calcite
X-1	6801.15	47	21	26	5	tr	tr	tr		tr	50		tr	
X-2	6802.18	40	25	27	3	tr	tr	tr		tr	N/A		3	
X-3	6809.00	37	34	22	3	tr	tr			tr	50		2	
X-4	6810.15	37	37	21	4	tr				tr	50		tr	
X-5	7442.60	62	3	2	15	2	16	1	tr				tr	tr
X-6	7445.40	56	2	1	12	1	24	2				3	1	tr
X-7	7447.95	38	27	24	4	tr	tr	tr		tr	50	1	4	
X-8	7451.85	42	36	18	3	tr	tr			tr	N/A	tr	tr	

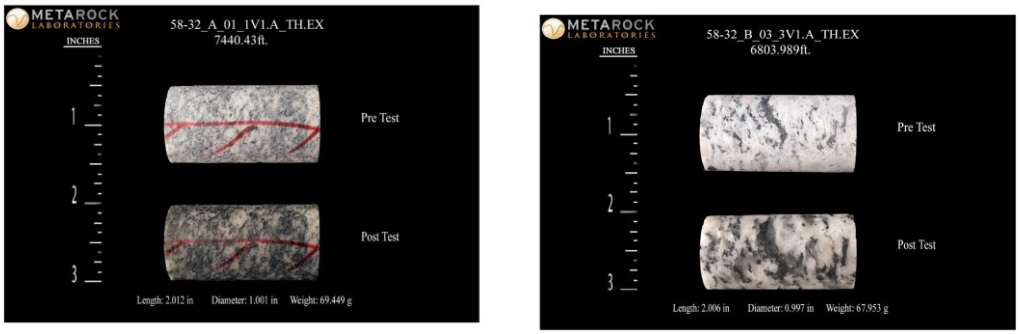

Figure 2: Photos of sample 58-32A and 58-32B from well 58-32 (MetaRock Laboratories, 2021).

2.2 Thermal properties measured from cuttings

Drilling cuttings were collected at 10-ft intervals from 100 to 7500 ft MD from well 58-32. Thermal conductivity was measured on the cutting samples at 100-foot intervals, as well as selected intermediate depths at room temperature (Gwynn et al., 2019). These measurements confirm the depth-dependent spatial heterogeneity of thermal conductivity. Within the reservoir range (5000 ft to 8000 ft), matrix thermal conductivity ranges from approximately 2.4 to 4.0 W/(K·m), varying by 67%. Below 6200 ft MD, thermal conductivity exhibits a general decreasing trend with increasing depth. Moreover, under reservoir condition, thermal conductivity is expected to decrease further with increasing depth due to elevated temperature. These cutting-based measurements also confirmed the conclusions drawn from core sample testing that the thermal conductivity around 6800 ft MD is greater than that around 7440 ft MD (refer to Figure 3). In Figure 3, bulk thermal conductivity is correspondingly less than the matrix thermal conductivity because the bulk measurement considers the porosity and water in the pores and the thermal conductivity of water is less than that of the rock.

These data also show a strong positive correlation between thermal conductivity and quartz abundance: higher quartz content consistently corresponds to higher conductivity (refer to Figure 4), consistent with observations from the core measurements. Samples with low quartz content are predominantly dioritic, whereas those with high quartz content are granitic.

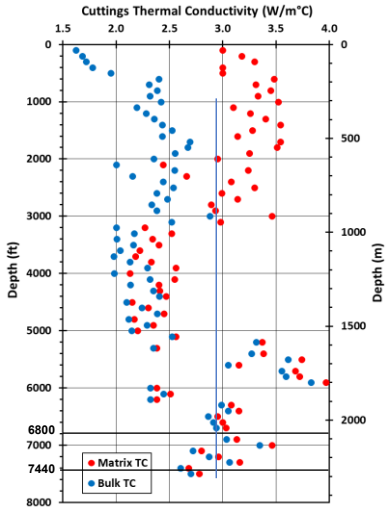

Figure 3: Thermal conductivity data for well 58-32 based on cuttings measurements (adapted from Gwynn et al., 2019) at room temperature.

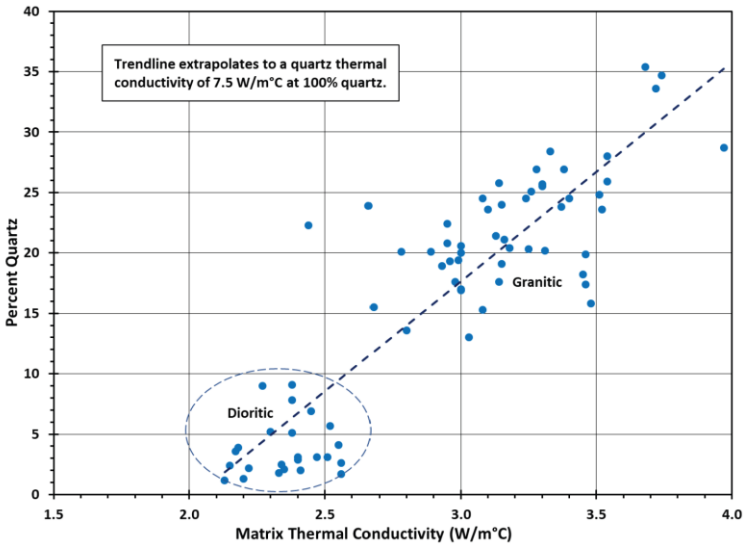

Figure 4: Quartz percentage vs. matrix thermal conductivity for cuttings from well 58-32 (adapted from Gwynn et al., 2019).

3. HEAT TRANSFER ANALYSIS

In this section, we investigate the influence of rock thermal properties on thermal production performance and fracture spacing of EGS using analytical solutions and numerical simulations. The numerical simulation was conducted using Itasca's XSite^{TM} (Itasca Consulting Group, 2024). We first examine the performance of single fracture system under different thermal properties, followed by an analysis

thermal production from a doublet system connected by multiple fractures. Finally, we evaluated the required fracture spacing to avoid heat interference under different thermal properties.

The range of rock thermal properties considered in this study is based on the measurement from core and cuttings from Utah FORGE wells as discussed in Section 3. For the high-thermal-property case, thermal conductivity is 3.0 W/(m·K), and specific heat is 1170 J/(kg·K), corresponding to sample 58-32B at 100 ºC characterized by a high quartz content. For the low-thermal-property case, thermal conductivity is 2.0 W/(m·K), and specific heat is 981 J/(kg·K), corresponding to 58-32A at 200 ºC with low quartz content. The thermal conductivity of the high-thermal-property case is 50% higher than the low-thermal-property case while the specific heat capacity is approximately 20% higher. This contrast considers both the influence of mineral content and temperature, and it is conservative as the variation of thermal conductivity from cuttings reaches up to 67%.

3.1 Single fracture system

Three cases are investigated for a doublet system connected by a single fracture: 1) homogeneous medium with high thermal properties, 2) homogeneous medium with low thermal properties, 3) heterogeneous medium consisting of a 20m-thick layer with high thermal properties sandwiched between two 40m-thick layers with low thermal properties.

For a single fracture in homogeneous medium, the output fluid temperature can be expressed (Lowell, 1976):

$$T_W(z,t) = T_{W0} + (T_{R0} - T_{W0})\,\mathrm{erf}\left[\frac{(K_R\rho_R c_R)^{\frac{1}{2}} z}{c_w \rho_w Q t^{\frac{1}{2}}}\right] \quad (1)$$

The injected fluid temperature T_{W0} is 50 ºC, the reservoir temperature is 210.2 ºC, fluid density ρ_R is 900 kg/m^3, fluid specific heat capacity as 4184 J/(kg·K), injection rate (per unit fracture length) Q is 1.78×10^{-5} m^2/s [the equivalent width H is 120 m], and rock density is 2650 kg/m^3. For the high-thermal-property case, the production temperature at $z = 100$ m is 170.6 ºC at the end of 12 months. In contrast, for the low-thermal-property case, the production temperature at $z = 100$ m is 148.2 ºC at the end of 12 months. This corresponds to a temperature difference of 15.1%. When a cutoff temperature of 65 °C is applied, the resulting a 26.9% increase in thermal power production.

Numerical simulations were conducted for these three cases described above. In the numerical models, the initial rock temperature at the center of the model is 206.2 ºC, and a geothermal gradient of 0.071 ºC/m is applied. The fracture dimensions are 250m×400m, with an aperture of 0.11 mm. The injection temperature is 50 ºC, and the injection rate is 0.8 bpm (0.00213 m^3/s). The fluid and rock properties are identical to those used in the analytical solution.

Figure 5a shows the simulated production temperature histories for the three cases with a single fracture. At the end of 12 months, the simulated production temperature of the high-thermal-property case is 335.5 ºF (168.6 ºC), which is close the corresponding analytical prediction considering equivalent fracture width L as 120 m. However, the simulated production temperature of low-thermal-property case – 316.6 ºF (158.1 ºC) is much higher than the prediction from Lowell's solution. The discrepancy between the analytical solution and the numerical results arises from differences in flow representation. The analytical solution assumes one-dimensional fluid flow, whereas the numerical model accounts for finite-volume injection and production zones, and two-dimensional radial flow within the fracture. When thermal diffusivity is lower, as in the low-thermal-property case, rock temperatures far from the injection center are less affected. This results in a lower effective injection rate and, correspondingly, a higher effective production temperature in the numerical simulations.

The simulated production temperature of low-thermal-property case is 18.9 °F (10.5 °C) less than the simulated result with high-thermal-property. Figure 5b shows the simulated produced thermal power with time, calculated using a cutoff temperature of 65 °C. The produced thermal power in the high-thermal-property homogenous case is 11.3% greater than that in the low-thermal-property case. In contrast, introducing a 20m-thick high-thermal-property layer within an otherwise low-thermal-property reservoir results in only a 3.5% increase in thermal power production relative to the homogeneous low-thermal-property case.

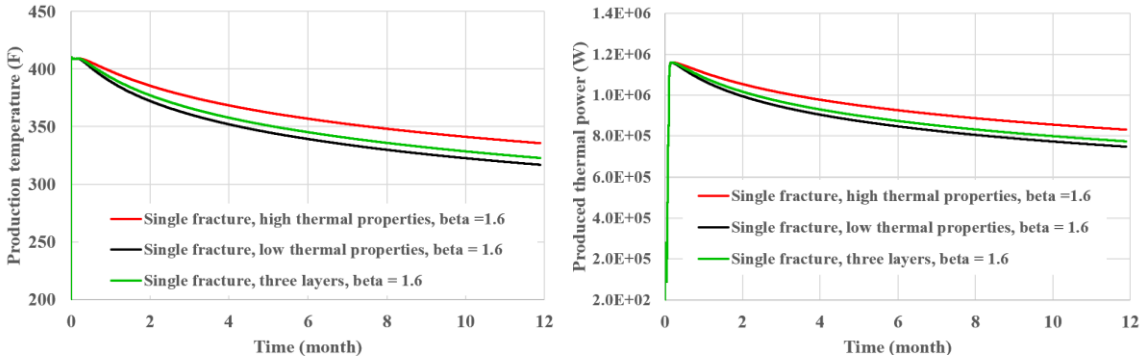

(a) Production temperature (b) Produced thermal power

Figure 5. Simulation results of the three cases with a single fracture: (a) production temperature, (b) produced thermal power.

Figure 6 shows the fluid temperature contours within the single fracture for these three cases. As expected, the fluid temperature in the high thermal properties layer is larger than the corresponding part in the homogenous low-thermal-property case.

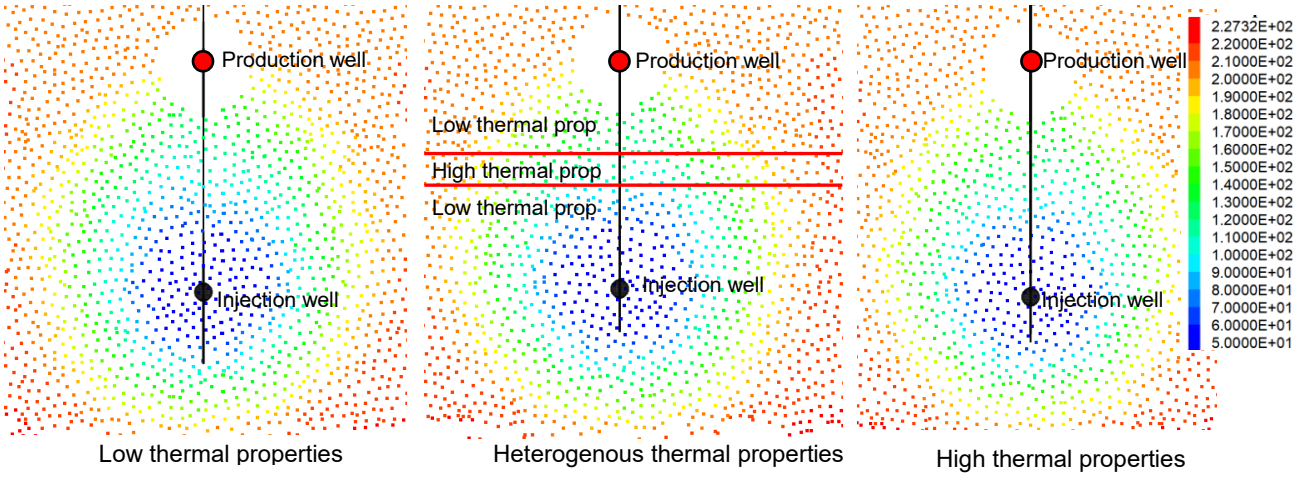

Figure 6. Fluid temperature contour at the end of 12 months circulation (a) homogeneous – low thermal conductivity and heat capacity; (b) heterogeneous – three layers with a high-thermal-property layer in the middel; (c) homogeneous - high thermal conductivity and heat capacity.

3.2 Multiple fractures system

The configuration of the doublet system connected by multiple fractures is illustrated in **Figure 7**, following the FORGE modeling framework described in Xing et al., 2025. Similar to the single-fracture analysis, three cases were investigated: 1) homogeneous medium with high thermal properties, 2) homogeneous medium with low thermal properties, 3) heterogenous medium consisting of a 130m-thick layer with high thermal properties sandwiched between two layers with low thermal properties (refer to **Figure 7**b). The injection rate is 8.8 bpm (0.0234 m3/s), equal to the effective injection rate during one-month circulation testing at Utah FORGE site in 2024, and the injected fluid temperature is 50 ºC at the fracture entry. The fracture aperture varies from 0.1 to 0.2 mm.

The history of production temperature of three multiple-fracture system cases is shown in Figure 8a. After 12 months of operation, the production temperature for the high-thermal-property case reaches 323.8 °F (162.1 °C), whereas the low-thermal-property case yields a production temperature of 307.0 °F (152.8 °C). For the three-layer heterogeneous case, the production temperature at 12 months is 312.8 °F (156.0 °C). The produced thermal power for the high-thermal-property case is 8.56 MW, which is 10.6% higher than the low-thermal-property case. Introducing a 130m-thick high-thermal-property layer results in a 3.6% increase in thermal power production relative to the homogeneous low-thermal-property case. The spatial distribution of fluid temperature within the fractures of the three-layer heterogenous case is shown in Figure 9.

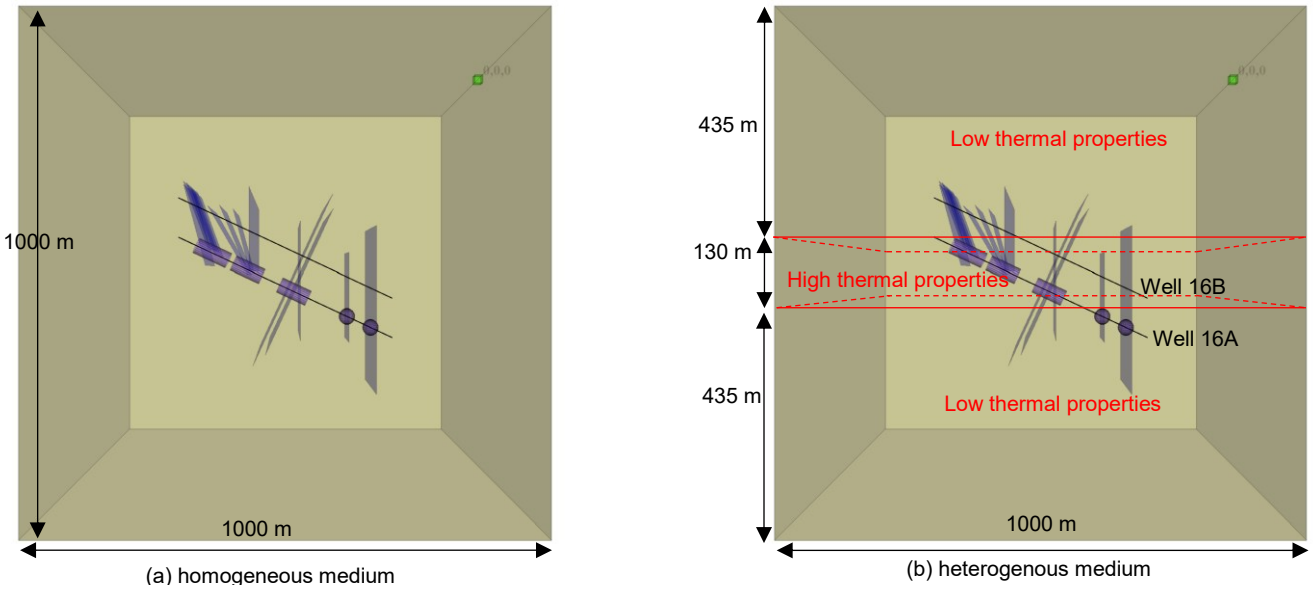

Figure 7. Configurations of the subsurface multiple fracture system: (a) homogenous medium, (b) heterogeneous medium consisting of a 130m-thick high-thermal-property layer sandwiched between two layers with low thermal properties.

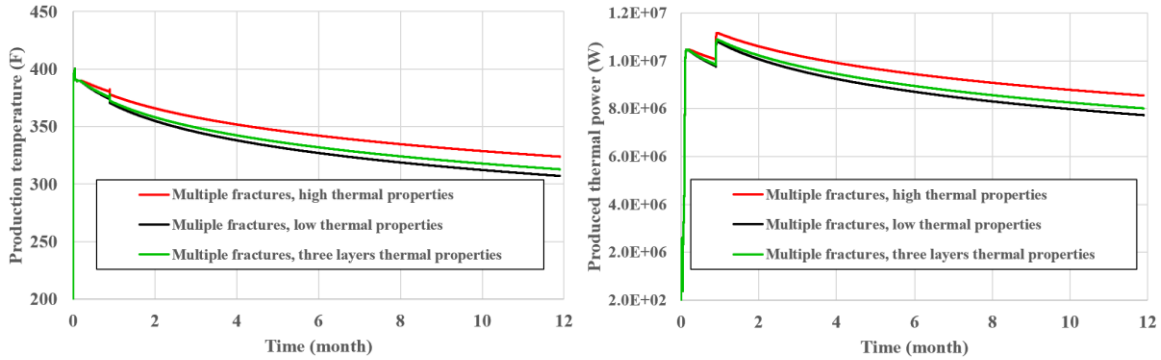

Figure 8. Simulation results of the three cases with multiple fractures: (a) production temperature, (b) produced thermal power.

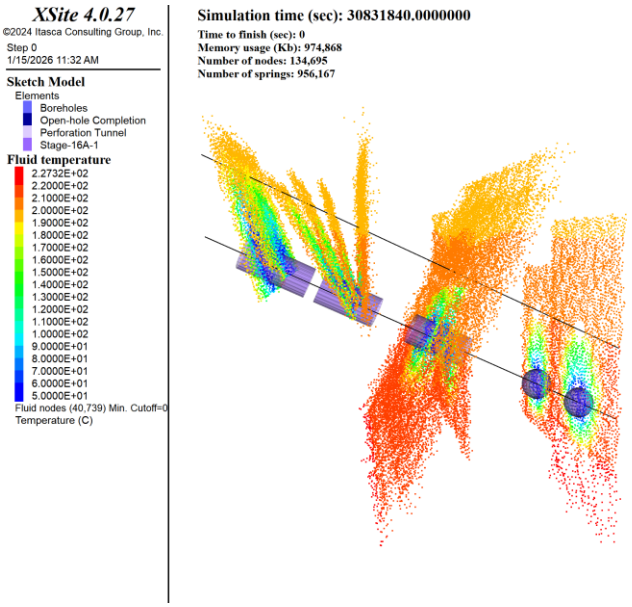

Figure 9. Fluid temperature contour in the fractures for the three-layer heterogeneous case at the end of 12-month circulation.

3.3 Fracture spacing

Fracture spacing is a key design parameter for hydraulic stimulation in EGS. If the fracture spacing is too large, the thermal energy stored in the reservoir will not be fully extracted; conversely, if fractures are spaced too closely, there will be thermal interference between adjacent fractures.

In order for the fractures to be considered thermally independent at a time t_o, the fracture spacing L must satisfy the following condition (Lowell, 1976):

$$L \geq 3\left(\frac{K_R t_o}{\rho_R c_R}\right)^{\frac{1}{2}} \tag{2}$$

This expression shows that the fracture spacing L is related to thermal diffusivity $K_R/(\rho_R c_R)$: larger thermal diffusivity requires larger fracture spacing to maintain thermal independence.

Figure 10 illustrates the required fracture spacing to avoid heat interference for two cases – low temperature condition and high temperature condition. For low-temperature condition, the thermal conductivity is 3.1 W/(K·m) and specific heat capacity as 988.2 J/(kg·K), corresponding to the thermal properties of core sample 58-32B at 35 °C (refer to Table 1). For high-temperature condition, the thermal conductivity decreases to 2.7 W/(K·m) (a reduction of 12.9%) while specific heat capacity increases to 1175.2 J/(kg·K) (an increase of 18.9%), corresponding thermal properties of the same sample at 200 °C. The density is 2650 kg/m^3 for both cases. Thus, the thermal diffusivity $K_R/(\rho_R c_R)$ decreases with increasing temperature, leading to a reduction on the required fracture spacing. This implies that required fracture spacing to avoid heat interference decreases with increasing depth due to rising temperature. As shown in **Figure 10**, the required spacing to avoid heat interference increase with the targeted production duration. For a typical geothermal power plant of 30 years life span, the required spacing to avoid heat interference for high-temperature condition is 85 m, which is 15 m less than the 100m required for low-temperature condition.

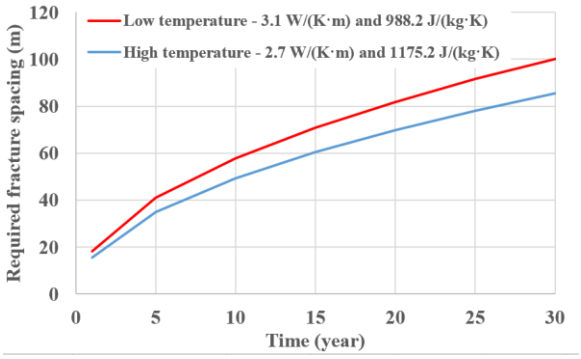

Figure 10. Required spacing to avoid heat interference for different temperature conditions. For the low-temperature condition: thermal conductivity is 3.1 W/(K·m) and specific heat capacity as 988.2 J/(kg·K); high-temperature condition: the thermal conductivity is 2.7 W/(K·m) and specific heat capacity as 1175.2 J/(kg·K).

4. CONCLUSIONS

The measurements from Utah FORGE core samples show that the thermal conductivity in the most conductive sample is ~50% higher than in the least conductive sample, while specific heat capacity is also ~20% higher. XRD analyses performed on the same core samples attribute these variations largely to differences in quartz content. Continuous thermal property measurements from drilling cuttings in well 58-32 at room temperature further confirm spatial heterogeneity, with thermal conductivity varying by up to 67% along depth. These measurements also show a strong positive correlation between thermal conductivity and quartz abundance: higher quartz content consistently corresponds to higher conductivity. Not only do the thermal properties vary with different mineral components, but they are also a function of temperature. The laboratory data shows that thermal conductivity decreases while specific heat capacity increases with increasing temperature, leading to a reduction in thermal diffusivity at elevated temperatures for constant density.

Numerical simulations were conducted to quantify the impact of thermal property variability on EGS thermal production performance. For a single-fracture system, a 50% increase in thermal conductivity combined with a 20% increase in heat capacity yields 18.9 ºF (10.5 ºC) increase in temperature and a 11.3% increase in thermal power production. For the FORGE-analog cases with multiple fractures, the corresponding temperature increase is about 16.7 ºF (9.3 ºC), while the thermal power production increases by 10.6%. In a heterogeneous reservoir scenario, introducing a 130m-thick layer with high thermal properties yields a 3.6% increase in thermal power production compared to the homogeneous low-thermal-property case.

Thermal property variations also influence fracture spacing requirements in EGS design. Because thermal diffusivity decreases with increasing temperature, the required fracture spacing for thermal independence is reduced at higher temperatures. For a typical geothermal power plant with a 30-year operational lifetime, the required fracture spacing to avoid heat interference under high-temperature conditions is approximately 85 m, which is 15 m smaller than the 100 m spacing required under low-temperature conditions.

Overall, these results demonstrate that incorporating realistic thermal property variations impacts predicted production temperatures, thermal power output, and subsurface rock temperature evolution, underscoring the importance of accounting for rock thermal property heterogeneity in accurate performance assessment and optimal design of EGS.

REFERENCES

Cho, W. J., Kwon, S., & Choi, J. W. (2009). The thermal conductivity for granite with various water contents. Engineering geology, 107(3-4), 167-171.

Gwynn, M., Allis, R., Hardwick, C., Jones, C., Nielsen, P., & Hurlbut, W. (2019). Compilation of rock properties from FORGE well 58-32, Milford, Utah. Geothermal characteristics of the Roosevelt hot springs system and adjacent FORGE EGS site, Milford, Utah, 169.

Heuze, F. E. (1983, February). High-temperature mechanical, physical and thermal properties of granitic rocks—a review. In International Journal of Rock Mechanics and Mining Sciences & Geomechanics Abstracts (Vol. 20, No. 1, pp. 3-10). Pergamon.

Horai, K. I. (1971). Thermal conductivity of rock-forming minerals. Journal of geophysical research, 76(5), 1278-1308.

Itasca Consulting Group, Inc., 2024, XSite (Version 4.0.27). Itasca Consulting Group, Inc., Minneapolis.

Jones, C., Simmons, S., & Moore, J. (2024). Geology of the Utah frontier observatory for research in geothermal energy (forge) enhanced geothermal system (egs) site. Geothermics, 122, 103054.

Lowell, R. P. (1976). Comments on theory of heat extraction from fractured hot dry rock by AC Gringarten, PA Witherspoon, and Yuzo Ohnishi. J. Geophysics. Res.;(United States), 81(2).

Nash, G., & Jones, C. (2018). Utah FORGE: X-Ray Diffraction Data. [Data set]. Geothermal Data Repository. Energy and Geoscience Institute at the University of Utah. https://doi.org/10.15121/1452734

MetaRock Laboratories (2021). Utah FORGE: Well 58-32 Granite Core Thermal Properties Test Results Report (Oct. 2021). [Data set]. Geothermal Data Repository. Energy and Geoscience Institute at the University of Utah. https://gdr.openei.org/submissions/1430

Walsh, J. B., & Decker, E. R. (1966). Effect of pressure and saturating fluid on the thermal conductivity of compact rock. Journal of Geophysical Research, 71(12), 3053-3061.

Xing, P., Damjanac, B., McLennan, J., & Moore, J. (2025, June). Numerical Simulation of the Circulation Tests in 2024 at the Utah FORGE Site. In ARMA US Rock Mechanics/Geomechanics Symposium (p. D031S036R001). ARMA.